actual openings in our experiments. This implies that the exit surface surrounding the aperture must also be involved in the reradiation process, as we already inferred from the existence of the dispersion relation. Nonetheless, we do not have uniform emission from an area as large as implied by the above estimate. If the structure surrounding the central aperture emitted light very weakly, could this contribute to explain the small observed angular divergence? Within the resolution limit of our apparatus, we cannot preclude the presence of some emission from the surface whose intensity diminishes rapidly as a function of lateral distance from the aperture. Given our optically thick film, the source of this emission can only come from scattering of the light emerging from the aperture. To test this possibility, we implemented a simple first-principle model based on interference in the far-field of light scattered at the center of each groove with a laterally variable emission intensity given by a curve fit to the experimental results (Fig. 3, inset). In our model, the phase of the emission at each groove is proportional to the distance travelled by the surface wave from its origin at the aperture. These SPs travel slightly slower than light in free space due to retardation by the metal and, as a consequence, emission normal to the surface occurs at a wavelength slightly larger than the period. With this model, we are able to reproduce the overall features of the observed angular divergence of Figs. 1D and 2D, as well as the dependence of directionality on wavelength (Fig. 3).

Perhaps the most non-intuitive aspect of this phenomenon is the fact that scattering at the grooves of only a small fraction of the light emerging from the aperture can create such a narrow beam by interference (*20*). Even though the emission remains heavily confined to the immediate vicinity of the sub-wavelength aperture, the secondary contribution from the surface plasmons launched and scattered on the exit surface narrows the divergence dramatically from that of a normal isotropic distribution. The coupling of the electromagnetic wave of the SP back to light follows the dispersion curve imposed by the periodic structure surrounding the aperture. In effect, the combination of the periodic corrugation momentum (G) and SP momentum (k_{sp}) on the exit side acts like a k-vector filter on the reradiated light (k_{out}) defining the permitted emission angle θ (i.e., $k_{out} \sin\theta = k_{out//} = k_{sp} \pm G$). As a result, in the linear symmetry of the slit configuration, off-axis beams can exist with wavelength-dependent angles. In the circular symmetry of the bull's eye structure, off-axis beams are forbidden by destructive interference; only beams normal to the surface can exist at a specific wavelength dictated by the corrugation period.

The micro-scaled metallic structures described here transmit light with a combination of low divergence, directionality and high efficiency. Their spectral and angular characteristics can be tailored over a wide range in a one-step lithographic process by corrugating the surface lateral to the propagation direction of the transmitted beam. Such devices can be thought of as miniature phased-array antennas in the optical regime, which can transmit or receive light along a specific direction for a given wavelength. Potential applications of these results include spatial and spectral multiplexing (i.e., rerouting of light according to wavelength), coupling in and out of fibers, and optimizing near-field devices for microscopy or data storage purposes. Furthermore, the diffraction-reducing properties of our structures might be applied to reducing the intrinsically high beam divergence of common optical devices such as light-emitting diodes (*21*) and semiconductor lasers (*22*). In summary, our findings show a unique path toward achieving photonic miniaturisation without the usual scaling limitations in the subwavelength regime, such as low transmittance and severe diffraction.

References and Notes

1. J. B. Pendry, *Science* **285**, 1687 (1999).
2. W. L. Barnes, *IEEE J. Lightwave Techn.* **17**, 2171 (1999).
3. S. C. Kitson, W. L. Barnes, J. R. Sambles, *Phys. Rev. Lett.* **77**, 2670 (1996).
4. J. R. Krenn *et al.*, *Phys. Rev. Lett.* **82**, 2590 (1999).
5. T. W. Ebbesen, H. J. Lezec, H. F. Ghaemi, T. Thio, P. A. Wolff, *Nature* **391**, 667 (1998).
6. H. F. Ghaemi, T. Thio, D. E. Grupp, T. W. Ebbesen, H. J. Lezec, *Phys. Rev. B* **58**, 6779 (1988).
7. D. E. Grupp, H. J. Lezec, T. Thio, T. W. Ebbesen, *Adv. Mater.* **11**, 860 (1999).
8. L. Martin-Moreno *et al.*, *Phys. Rev. Lett.* **86**, 1114 (2001).
9. A. Krishnan *et al.*, *Opt. Lett.* **200**, 1 (2001).
10. E. Popov, M. Neviere, S. Enoch, R. Reinisch, *Phys. Rev. B.* **62**, 16100 (2000).
11. J. A. Porto, F. J. Garcia-Vidal, J. B. Pendry, *Phys. Rev. Lett.* **83**, 2845 (1999).
12. L. Salomon, F. Grillot, A. V. Zayats, F. de Fornel, *Phys. Rev. Lett.* **86**, 1110 (2001).
13. S. Collin, F. Pardo, R. Teissier, J.-L. Pelouard, *Phys. Rev. B* **63**, 033107 (2001).
14. V. A. Shubin, A. K. Sarychev, J. P. Clerc, V. M. Shalaev, *Phys. Rev. B* **62**, 11230 (2000).
15. J. M. Vigoureux, *Opt. Commun.* **198**, 257 (2001).
16. P. T. Worthing, W. L. Barnes, *Appl. Phys. Lett.* **79**, 3035 (2001).
17. A. P. Hibbins, J. R. Sambles, C. R. Lawrence, *J. Appl. Phys.* **87**, 2677 (2001).
18. J. J. Greffet *et al.*, *Nature* **416**, 61 (2001).
19. E. Hecht, *Optics* (Addison-Wesley, Reading, MA, 1990).
20. A detailed theoretical analysis of the phenomena is beyond the scope of this report and will be presented in a forthcoming paper.
21. A. Köck, E. Gornik, M. Hauser, W. Beinstingl, *Appl. Phys. Lett.* **57**, 2327 (1990).
22. T. Erdogan *et al.*, *Appl. Phys. Lett.* **60**, 1921 (1992).

23. The near-field experiments were carried out in the Submicron Optics Laboratory of the University of Burgundy, and the authors are grateful for the assistance of Y. Lacroute, C. Chicanne, and A. Dereux. The assistance of Andreas Schertel (FEI Europe) as well as valuable discussions with T. Thio (NECI) are also gratefully acknowledged.

15 March 2002; accepted 28 May 2002
Published online 20 June 2002;
10.1126/science.1071895
Include this information when citing this paper.

Femtosecond Infrared Spectroscopy of Bacteriorhodopsin Chromophore Isomerization

Johannes Herbst, Karsten Heyne,* Rolf Diller†

The vibrational dynamics of the retinal chromophore all-trans–to–13-cis photoisomerization in bacteriorhodopsin has been studied with mid-infrared absorption spectroscopy at high time resolution (about 200 femtoseconds). After photoexcitation of light-adapted bacteriorhodopsin, the transient infrared absorption was probed in a broad spectral region, including vibrations with dominant C–C, C=C, and C=NH stretching mode amplitude. All photoproduct modes, especially those around 1190 reciprocal-centimeters that are indicative for a 13-cis configuration of the chromophore, rise with a time constant of ~0.5 picosecond. The results presented give direct vibrational-spectroscopic evidence for the isomerization taking place within 0.5 picosecond, as has been suggested by previous optical femtosecond time-resolved experiments but questioned recently by picosecond time-resolved vibrational spectroscopy experiments.

Bacteriorhodopsin (bR) is a light-driven proton pump that has served as a model system for the study of protein-based, ultrafast, light-induced trans-cis isomerizations. It represents an entire class of retinal-containing proteins with similar photochemistry but very different biological functions, such as visual transduction in rhodopsin, chloride pump in halorhodopsin, and photoreception in sensory rhodopsin (*1*). In all of these seven-helical transmembrane proteins, a retinal chromophore is covalently bound by a protonated Schiff base (SB) to a lysine (Lys) residue. Photons electronically excite the chromophore and drive a C=C double-bond isomerization, which in bR transforms the all-trans into the 13-cis configuration.

Photoisomerization initiates a series of

thermally driven reaction steps that take place on a time scale up to milliseconds and are optimized in each system for the respective biological function. Even the respective primary photoreactions are optimized, which becomes clear when the primary photoreaction of the various rhodopsins are compared with that of the chromophore in solution (*2*). Details of initial reaction steps have been revealed by femtosecond time-resolved optical laser spectroscopy, which probes the transient absorption of the participating electronic states (*3*–*5*). This technique can now be done with extremely high time resolutions of about 30 fs (*6*) and even 5 fs (*7*). For bR, these studies have led to insights into the very fast processes on the excited electronic state surface. It is believed that, after excitation of the non-isomerized, light-adopted ground state of bR (br_{570}), fast relaxation along high-frequency (C–C) stretching modes depopulates the Franck Condon region before torsional movement. This model is corroborated by model calculations (*6*, *8*). According to the commonly accepted model (*3*, *4*), the transition of the excited electronic state S_1 to the first product electronic ground state (J) occurs within about 0.5 ps. Via vibrational cooling and torsional relaxation, the K state is formed within a few picaseconds (*9*), which then decays on a time scale of microseconds. The J and K states have red-shifted absorption bands with respect to bR_{570}. On the basis of comparative studies on the native system, bR, and a bR analog containing a sterically all-trans locked retinal (*10*, *11*), the indication for J being a 13-cis state that formed directly from the excited electronic state within about 500 fs was recently questioned.

Despite their high temporal resolution, optical transient absorption experiments do not provide direct information about structural dynamics, which can be obtained from time-resolved resonance Raman (RR) or infrared (IR) spectroscopy. Important results concerning the chromophore structure in the early K state were already obtained by time-resolved RR spectroscopy. With pulses of 1 ps or less (*12*, *13*), it was possible to obtain RR spectra of precursor states of K that indicated a 13-cis configuration of the chromophore (*13*). However, time-resolved coherent anti-Stokes Raman scattering (CARS) experiments (*11*) suggested that all-trans–to–13-cis isomerization takes place later than J formation and possibly as late as K formation.

So far, the structural dynamics of chromophore isomerization in bR have not been investigated at sufficient temporal and spectral resolution to time-resolve those features in the vibrational spectrum that identify the formation of the isomerized 13-cis product. We directly address and answer questions concerning the timing of the chromophore isomerization and its relation to the decay of the excited electronic state and the formation of the electronic ground state (S_0) as raised in Ahroni *et al.* (*10*) and Atkinson *et al.* (*11*). The direct marker bands for the all-trans–to–13-cis isomerization in the 1200 cm^{-1} spectral region, together with C=C and C=NH stretch vibrations, were monitored by transient optical-pump–IR-probe spectroscopy at a time resolution better than 230 fs, sufficient to resolve the dynamics on the time scale believed to govern the S_1-S_0 transition. The spectral resolution varies between 3 and 5 cm^{-1} and is also sufficient to resolve the chromophore vibrational bands of about 12 to 18 cm^{-1} full-width at half-maximum (FWHM).

We obtained high time resolution by using nonlinear optical methods. By difference frequency mixing in various steps, mid-IR pulses of 170 fs duration (FWHM) or shorter were generated at a repetition rate of 0.7 kHz. Simultaneously, laser pulses of 150 fs duration at 570 nm were generated and used to photoexcite the sample in the absorption maximum of the light-adapted electronic ground state bR_{570} to initiate the photoreaction. The transient absorption was probed by the mid-IR pulses at various delay times with respect to the excitation laser pulse at a system response function of ~230 fs FWHM (cross-correlation between pump and probe pulse). Because the probe wave number includes the region around 1600 cm^{-1}, where bulk water absorption is very strong, most of the water must be removed from the sample. We prepared a film of bR on a calcium fluoride (CaF_2) window, hydrated just sufficiently to ensure full protein stability and function and to avoid unnecessary absorption losses by water. Still, the photoinduced IR difference signals are small [on the order of a few thousandth optical density units (mOD)] compared with the huge absorption background caused by the protein vibrational bands (~1 OD) and residual water. The high repetition rate and the ms lifetime of the bR photocycle require that the sample film be moved across the focused laser beams in order to avoid multiple excitation of a specific sample volume. Thus, the sample film must be highly homogenous.

Structural changes initiated by the photoexcitation are reflected by changes in the vibrational spectrum of the chromophore. Selected IR transients (absorbance difference between pumped and unpumped sample) between –2.5 and 6 ps were taken in three important IR spectral regions, including the chromophore C=NH stretch vibrational mode around 1640 cm^{-1} (Fig. 1A), the C=C (ethylenic) stretch around 1530 cm^{-1} (Fig. 1B), and the C–C stretch (fingerprint) around 1200 cm^{-1} (Fig. 1C) (*14*). IR difference spectra are also shown for an overview, taken at delay times of 1 (Fig. 2A) and 12 ps (Fig. 2B), and for comparison a Fourier-transform infrared (FTIR) spectroscopy step-scan bR_{570}-K difference spectrum (Fig. 2C), taken at 15-ns time delay (*15*). Difference spectra of the marker band region around 1200 cm^{-1} at various delay times are given in Fig. 3.

At positive delay times, the signals are composed of contributions from the transient molecular species participating in the photoreaction. Positive signals are caused by vibrational transitions generated at the respective spectral position by photoexcitation, whereas negative signals are caused by vibrational transitions removed from the respective spectral position by photoexcitation. The IR tran-

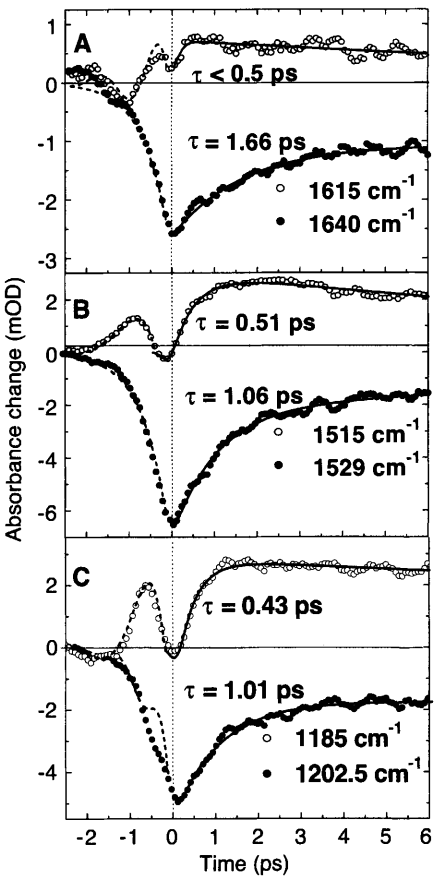

Fig. 1. Selected IR transients of bR (taken at room temperature with excitation at 570 nm) in (**A**) the region of the chromophore C=NH stretch vibration around 1640 cm^{-1}, (**B**) the ethylenic C=C stretch region around 1530 cm^{-1}, and (**C**) the fingerprint region with C–C stretch vibrations around 1200 cm^{-1}. τ, time constant of bleach recovery and rise of the positive signals, respectively, as fitted (solid line) by a sum of exponentials, convoluted with the system response function. At negative delay times, the signals are modeled according to (*16*), shown by dashed line.

Institut für Experimentalphysik, Freie Universität Berlin, Arnimallee 14, 14195 Berlin, Germany.

*Present address: Max-Born-Institut, Max-Born-Straße 2A, 12489 Berlin, Germany.

†To whom correspondence should be addressed. E-mail: diller@physik.fu-berlin.de

sients shown were fitted by a sum of exponentials convoluted with the system response.

In contrast, at negative delay times the signals are due to a coherent phenomenon (perturbed free-induction decay) caused by the IR probe pulse interacting with a vibrational transition before the pump pulse. If the probe pulse overlaps spectrally with a vibrational transition, it induces a polarization that emits in the probe pulse direction and decays with the dephasing time T_2 of the vibrational transition (that is, the inverse of its spectral width; a line width between 10 and 20 cm^{-1} corresponds to T_2 between about 1 and 0.5 ps). If the transition remains unaffected by the following pump pulse, there is no net effect in the detected IR difference signal. However, if the transition is affected in spectral position or absorption cross section, then the effect manifests as an oscillatory signal in time and frequency domain. On resonance, when the probe frequency coincides with the center frequency of the transition and the transition is spectrally separated from the probe pulse by the photoexcitation, the resulting negative signal (bleach) appears with the time constant T_2 (Fig. 1, A and B). Vibrational transitions that are generated by photoexcitation at the probe wavelength (positive signals) appear with a time constant determined by the intrinsic rate of formation and the system response. This effect is known from optical spectroscopy concerning electronic and vibrational transitions, and the presented kinetic curves were modeled accordingly (*16*).

Analysis of the IR transients at positive delay times yielded rise time constants of about 0.5 ps for all positive signals shown, followed by a very small decay with a much longer time constant. The negative signals rise as determined by the coherent effect and decay partially with a time constant between 1 and 1.7 ps. This effect is also reflected in the difference spectra (Fig. 2) at 1 and 12 ps by the respective negative signal amplitudes.

In the fingerprint region around 1200 cm^{-1}, C–C stretching vibrations serve as crucial marker bands for the chromophore configuration, that is, all-trans or 13-cis, as shown by RR and IR spectroscopy of isotopically labeled chromophores and normal mode calculations (*14*, *17*–*19*). In the K state, the chromophore is in 13-cis configuration. Bleaching bands were observed (Figs. 2 and 3) at 1170 and 1200 cm^{-1}, as expected for the all-trans chromophore, and a product band rose at 1190 cm^{-1}, with a small shoulder at 1180 cm^{-1}. This difference pattern is typical of the configurational change from all-trans to 13-cis that also has been found in the step-scan FTIR bR_{570}-K difference spectrum taken at 15 ns and ambient temperature (*15*) (Fig. 2C) and in time-resolved RR spectra (*20*, *21*).

The strong signals around 1530 cm^{-1} have been assigned to an in-phase C=C stretching vibration of the chromophore. Its position reflects the π-electron delocalization in the polyene part of the chromophore; a smaller wave number corresponds in a linear dependency (*13*, *22*) to a red-shifted optical absorption maximum (λ_{max}) of the respective intermediate state of the bR photocycle. The initial bleach occurs at 1529 cm^{-1}, as expected for bR_{570}. Positive signals appear at lower energies around 1515 cm^{-1}, indicating a red-shifted λ_{max}.

The region around 1630 cm^{-1} is dominated by strong signals due to the C=NH stretch vibration of the chromophore. This mode is sensitive to the environment of the SB linkage between the retinal chromophore and Lys^{216}. The bleach signal appears as expected at 1640 cm^{-1}, the position of the C=NH stretch vibration in bR_{570}. Product signals rise between 1620 and 1600 cm^{-1}. The observations concerning the C=NH and C=C region are consistent with earlier results (*23*–*25*) performed at lower time resolution and with a different experimental technique. All together, the overview difference spectra shown in Fig. 2, A and B, look much like the FTIR bR_{570}-K difference spectrum given in (*15*) and shown in Fig. 2C. Differences in the relative band intensities between Fig. 2, A and B, are due to the partial recovery of the bR_{570} ground state, which is not complete after 1 ps (Fig. 2A).

The fast rise of the positive vibrational bands (Fig. 1; Fig. 2, A and B) and the comparison with the FTIR difference spectrum (Fig. 2C) show that within 500 fs the retinal chromophore (i) assumes 13-cis configuration, (ii) exhibits a red-shifted (J) λ_{max} in line with optical transient absorption experiments, and (iii) experiences a changed SB environment. These jointly consistent observations show that isomerization takes place within 500 fs and not later, in variance with the conclusions by Atkinson *et al.* (*11*). Furthermore, they show that isomerization follows a similar time dependence as the S_1-S_0 transition; that is, isomerization is related to the excited electronic state decay and J formation, as suggested by various groups using optical transient absorption spectroscopy. The typical all-trans–to–13-cis difference pattern exists already at the early stages of the photoinduced transformation, as indicated in the early difference spectra of the fingerprint region (Fig. 3).

The J-K transition is not easily observed in the single kinetic traces, but a single-value decomposition analysis of the whole data set (*26*) revealed a 3-ps component associated with a K-like difference spectrum.

In contrast to the fast-rising product bands (0.5 ps), the bleach signals decay partially within 1.0 to 1.7 ps (Fig. 1; Fig. 2, A and B). This incomplete decay is predominantly due to the fraction of the excited state population that is fed back to the bR_{570} ground state according to the bR reaction quantum yield of 0.64 (*27*, *28*). The apparent amount of recovery is determined by the spectral overlap of the (negative) bR_{570} ground state and (positive) product bands. The observed recovery is faster than K formation (3 ps) but slower than product formation. This result indicates that the product (J) and the recovering educt (bR_{570}) are not directly populated from the same state. If we assume a homogenous bR_{570} ground state distribution, this result can be explained either by an early branching

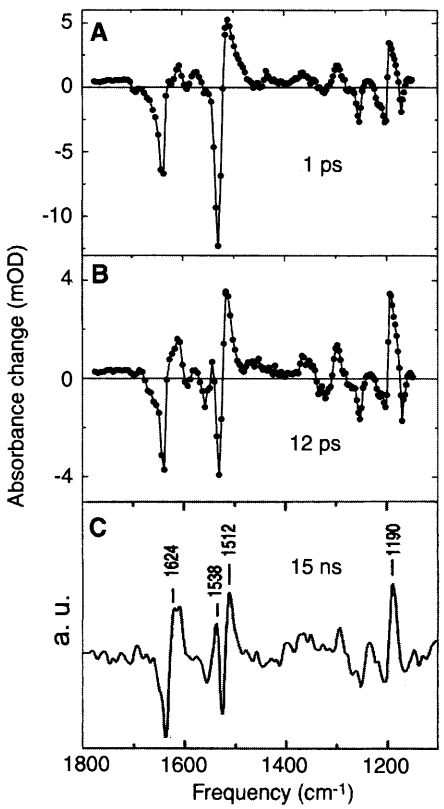

Fig. 2. IR difference spectra of bR with conditions as in Fig. 1 at (**A**) 1 ps and (**B**) 12 ps. (**C**) For comparison, a FTIR bR_{570}-K difference spectrum at 15 ns after photoexcitation at room temperature [from (*15*)].

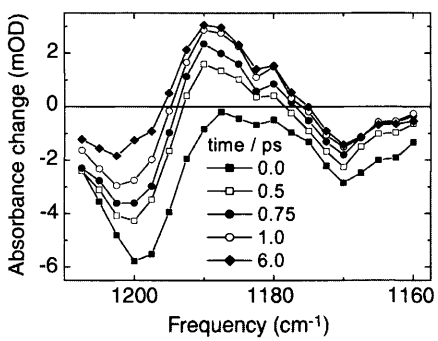

Fig. 3. IR difference spectra of bR with conditions as in Fig. 1 in the fingerprint region. The product band has a uniform rise around 1190 cm^{-1} with a shoulder at 1180 cm^{-1} indicating the 13-cis configuration of the chromophore.

reaction in S_1 (model A) or by a multi-stepwise recovery of the bR_{570} ground state within S_0 (model B). Indications for model A were given from the observation of a biphasic decay of the excited electronic state with time constants of 0.24 and 0.75 ps (*5*). These authors suggested a fast, reactive path leading to the isomerized state (J) and a slower, nonreactive path leading back to the educt. This model cannot be ruled out by the IR transients reported here, which rise within 0.5 ps or less; however, it is not supported by our own optical experiments (*26*).

The more likely model is model B, which could be realized by vibrational relaxation (for example, vibrational cooling) processes in S_0 that accompany the full recovery to the vibrational ground state of bR_{570} within 1.0 to 1.7 ps and the transformation from J to K in 3 ps. The J-K transition might take longer than the bR_{570} recovery because substantial conformational changes, including parts of the protein, are involved in the former. Vibrational cooling would be indicated by the decay of small shoulders on the low-energy side of the vibrational bands as the vibrational ground state recovers, an effect which is easily obscured by the 13-cis product bands. However, this view is also supported by time-resolved IR experiments on the isomerization reaction of protonated SB retinal in solution (*29*) and the observation of anti-Stokes RR bands of the chromophore in bR (*20*, *30*).

A small negative shoulder at about 1660 cm^{-1} (Fig. 2, A to C) appears within 1 ps or less (the apparent rise time is again limited by the dephasing time). Because no chromophore vibrational band is expected in this spectral region, it is possibly a contribution of the protein amide I band or a result of the bending vibration of a protein-bound water molecule. The molecular structure of bR as determined from x-ray diffraction (*31*) indicates a water molecule close to the SB as part of the hydrogen bond network in the chromophore binding pocket. Photoexcitation, that is, an electric field jump, or isomerization of the chromophore, might affect the absorption cross section, orientation, or even location of this water molecule or of a protein constituent and may lead to the observed bleach signal. In this case, the observed signal would indicate a fast response not of the chromophore but of the environment, that is, the cofactor binding pocket.

References and Notes

1. For reviews about retinal proteins, see: *Isr. J. Chem.* **35** (nos. 3 and 4) (1995).
2. P. Hamm *et al.*, *Chem. Phys. Lett.* **263**, 613 (1996).
3. J. Dobler, W. Zinth, W. Kaiser, D. Oesterhelt, *Chem. Phys. Lett.* **144**, 215 (1988).
4. R. Mathies, C. H. B. Cruz, W. T. Pollard, C. V. Shank, *Science* **240**, 777(1988).
5. F. Gai, K. C. Hasson, J. Cooper McDonald, P. A. Anfinrud, *Science* **279**, 1886 (1998).
6. W. Zinth *et al.*, *Springer Ser. Chem. Phys.* **66**, 680 (2000).
7. T. Kobayashi, T. Saito, H. Ohtani, *Nature* **414**, 531 (2001).
8. M. Garavelli, F. Negri, M. Olivucci, *J. Am. Chem. Soc.* **121**, 1023 (1999).
9. H.-J. Polland *et al.*, *Biophys. J.* **49**, 651 (1986).
10. A. Ahroni *et al.*, *Biochemistry (Moscow)* **66**, 1210 (2001).
11. G. H. Atkinson, L. Ujj, Y. Zhou, *J. Phys. Chem. A* **104**, 4130 (2000).
12. L. Song, M. A. El-Sayed, *J. Am. Chem. Soc.* **120**, 8889 (1998).
13. R. van den Berg, D. J. Jang, H. C. Bitting, M. A. El-Sayed, *Biophys. J.* **58**, 135 (1990).
14. S. O. Smith *et al.*, *J. Am. Chem. Soc.* **109**, 3108 (1987).
15. Reprinted with the permission of F. Siebert and the Biophysical Society, from C. Rödig, I. Chizhov, O. Weidlich, F. Siebert, *Biophys. J.* **76**, 2687 (1999).
16. P. Hamm, *Chem. Phys.* **200**, 415 (1995).
17. M. Braiman, R. A. Mathies, *Proc. Natl. Acad. Sci. U.S.A.* **79**, 403 (1982).
18. B. Curry *et al.*, *Adv. Infrared Raman Spectrosc.* **12**, 115 (1985).
19. S. O. Smith, J. A. Pardoen, J. Lugtenburg, R. A. Mathies, *J. Phys. Chem.* **91**, 804 (1987).
20. S. J. Doig, P. J. Reid, R. A. Mathies, *J. Phys. Chem.* **95**, 6372 (1991).
21. R. Lohrmann, I. Grieger, M. Stockburger, *J. Phys. Chem.* **95**, 1993 (1991).
22. L. Rimai, M. E. Heyde, D. Gill, *J. Am. Chem. Soc.* **95**, 4493 (1973).
23. R. Diller *et al.*, *Chem. Phys. Lett.* **241**, 109 (1995).
24. R. Dziewior, R. Diller, *Ber. Bunsenges. Phys. Chem.* **100**, 2103 (1996).
25. R. Diller, *Chem. Phys. Lett.* **295**, 47 (1998).
26. J. Herbst, K. Heyne, R. Diller, unpublished data.
27. J. Tittor, D. Oesterhelt, *FEBS Lett.* **263**, 269 (1990).
28. G. Schneider, R. Diller, M. Stockburger, *Chem. Phys.* **131**, 17 (1989).
29. P. Hamm *et al.*, *Chem. Phys. Lett.* **268**, 180 (1997).
30. T. L. Brack, G. H. Atkinson, *J. Phys. Chem.* **95**, 2351 (1991).
31. H. Luecke, B. Schobert, H. T. Richter, J. P. Cartailler, J. K. Lanyi, *J. Mol. Biol.* **291**, 899 (1999).

32. Valuable discussions with M. Sheves and M. Ottolenghi are greatly acknowledged. We thank D. Stehlik for support, M. Heyn and I. Wallat for generous bR sample supply, and U. Alexiev for characterizing the ms kinetics of the bR films. Supported by Deutsche Forschungsgemeinschaft Sfb 450.

22 March 2002; accepted 5 June 2002

Crystallographic Evidence for a Free Silylium Ion

Kee-Chan Kim,[1] Christopher A. Reed,[1*] Douglas W. Elliott,[1] Leonard J. Mueller,[1] Fook Tham,[1] Lijun Lin,[2] Joseph B. Lambert[2*]

Evidence for a three-coordinate silyl cation is provided by the crystal structure of $[(Mes)_3Si][H\text{-}CB_{11}Me_5Br_6]\cdot C_6H_6$ (where Mes is 2,4,6-trimethylphenyl). Free $(Mes)_3Si^+$ cations are well separated from the carborane anions and benzene solvate molecules. *Ortho*-methyl groups of the mesityl substituents shield the silicon atom from the close approach of nucleophiles, while remaining innocent as significant ligands themselves. The silicon center is three-coordinate and planar. The downfield ^{29}Si nuclear magnetic resonance chemical shift in the solid state (226.7 parts per million) is almost identical to that in benzene solution and in "gas phase" calculations, indicating that three-coordination can be preserved in all phases.

The silylium ion problem has exercised the minds of many (*1*–*5*). The essential debate concerns the existence of three-coordinate silicon cations, R_3Si^+ (where R is an alkyl or aryl group), unfettered by interactions with solvent, counterion, or neighboring groups. The fundamental question concerns how far the analogy to carbocations, R_3C^+, known now for more than 100 years (*6*), extends down group 14 of the periodic table.

Despite ready mass spectrometric detection in the gas phase, there has been no convincing evidence for the existence of free R_3Si^+ ions in condensed phases when R is an alkyl group. The closest approach is found in "ion-like" species, $R_3Si^{\delta+}Y^{\delta-}$, where R is *iso*-propyl and Y is a very weakly coordinating anion, such as the perfluorinated tetraphenylborate ion or a carborane (*7*). These species behave like silylium ions toward arenes (*8*) and in the production of superacidity (*9*), but they are not free silylium ions.

However, when R is a bulky aryl group, there is growing spectroscopic evidence and theoretical support for truly free, three-coordinate silyl cations. Species formulated as $[Ar_3Si][Y]$ have been reported for Ar = mesityl or duryl and $Y = B(C_6F_5)_4^-$ (*10*, *11*). Silyl cation character is indicated by downfield shifted resonances in the ^{29}Si nuclear magnetic resonance (NMR) spectrum near 220 parts per million (ppm). The NMR shifts have been reproduced computationally in the calculated structures of these triarylsilylium ions (*12*, *13*). An arylated silatropilium ion (*14*) and a *cyclo*-tetrasilenylium ion with bulky substituents (*15*) provide convincing evidence for three-coordination in other sili-

[1]Department of Chemistry, University of California, Riverside, CA 92521–0403, USA. [2]Department of Chemistry, Northwestern University, 2145 Sheridan Road, Evanston, IL 60208–3113, USA.

*To whom correspondence should be addressed. E-mail: chris.reed@ucr.edu (C.A.R.); jlambert@northwestern.edu (J.B.L.)